Journal of Advanced Zoology
ISSN: 0253-7214
Volume 45 Issue S-1 Year 2024 Page 297-310

Numerical And Analytical Study Of Unsteady Arterial Blood Flow In Time-Dependent Stenosis Using The Non-Newtonian Power-Law Blood Fluid Flow Model

Subrata Rakshit[1*], Bhawna Agrawal[2] , Sanjeet Kumar[3]

[1*,2]*Department of Mathematics, Rabindranath Tagore University, Bhopal, India, rakshit.subrata1983@gmail.com, bhawnakhushiagrawal@gmail.com*
[3]*Department of Mathematics Lakshmi Narain College of Technology & Science, Bhopal (M.P), India, sanjeetkumarmath@gmail.com*

***Corresponding Author:** Subrata Rakshit*
**Department of Mathematics, Rabindranath Tagore University, Bhopal, India, rakshit.subrata1983@gmail.com, bhawnakhushiagrawal@gmail.com*

Abstract:

This study tests the traits of shaky ancestry flow in a channel accompanying an occasion reliant blockage utilizing the Power-Law fluid model. Mathematical and computational models are grown to decide the chief order flow speed, pressure slope, resistance and divider clip stress at the throats and at the fault-finding crest of the blockage and we interrogate reliance of these quantities on the momentary and dimensional variables in addition to on the repetitiveness of the flow swinging sooner than expected and the main limits of the flow order. We find that as the proportion of blockage raised accompanying period and commonness, the principles of the size of the main speed, the resistance and the obstruction cut stress in the blockage district raised. We still find that magnitudes of these quantities are greater for the Newtonian fluid than for non-Newtonian fluid.

Keywords: Pressure Slop, Blockge, Unsteady Stenosis, Power-Law Fluid Model, Blood Flow, non-Newtonian Fluid, Artery Flow.

1. INTRODUCTION:

The stream through stenosed vessels would provide the plausibility of diagnosing the illness in its earlier stages, making treatment conceivable indeed some time recently the stenosis gets to be clinically noteworthy. As of now we do not have point by point information of stream design in an supply route with a stenosis. They happen due to the store of the cholesterol, greasy substance, cellular squander items, calcium and fibrin within the inward lining of an artery.

Many experimental studies reveal that in the vicinity of a stenosis, the shear rate of blood is low and therefore the non-Newtonian behavior of blood in that region is quite prominent. Young (1968), Young and Tsai (1973), Morgan and Young (1974) , and MacDonald (1979) have discussed some characteristics of flow of blood in stinted arteries by considering the blood flow as a steady Newtonian fluid. Many researchers consider that blood flow behaves as a non-Newtonian fluid inside a constricted artery. Furthermore, Hershey et al. (1964), Charm et al. (1974), Huckabe and Hahn (1968) have suggested that blood flow less than 20 s^{-1} shear rate in small diameter tubes (less than 0.2) can be represented by a Power-Law fluid model.

Hershey et al. (1964), Merrill (1965), Pedley and Berger (1980) and Jou (2000) have shown that at low shear rates the blood flow behaves like a non-Newtonian character in narrow vessels (radius less than 1 mm).

Mandal et al. (2005) have inspected the charactertics of blood of stream utilizing distinctive formed stenoses and watched that the blood stream experienced much higher resistance with a cosine shaped stenosis than the sporadic, smooth and deviated models.
In this paper, we consider the issue of shaky blood stream through an course with modern composite sine formed time subordinate stenosis and examine the characteristics of the blood stream utilizing the Power-Law fluid demonstrate, one of the trustworthy models, to recreate supply route blood stream. The axial velocity, pressure gradient, wall shear stress and impedance (flow resistance) are used to analyze unsteady blood flow in an artery using prescribed volume flow rate in contrast to other works using prescribed pressure gradient.

2. MATHEMATICAL MODEL

A mathematical model is an abstract description of a concrete system using mathematical concept and language. We recall the hassle of unsteady axisymmetric flow of blood in an artery in the shape of a round cylindrical tube of radius R_0 and within the presence of a time structured stenosis. The duration of the artery is assumed to be large in assessment to its radius R_0, so that the give up results can be left out. The interior Boundary of the tube is partly established alongside a distance L_0 due to the presence of a stenosis. The Blood float machine and the geometry are as shown (determine 1) in one on the spot in time. The arterial tube is given over a distance $2d + L_0$ within the axial route, d is the most peak of the stenosis. The critical Peak of the stenosis $3\delta/4$ is located at a distance $z = d + L_0/2$ from the origin of the coordinate device. Figure 2 indicates the geometrical form of the stenosis at onare of a kind time.
The commanding equatings for bulk preservation and impetus are second hand for the ancestry flow structure, and a Power-Law fluid model is secondhand for the vital stickiness. We deem the non-spatial form the governing spatial form of the governing for ancestry flow in the axisymmetric form and use tubular standards for judging or deciding with r as the branching changeable, z as the principal variable and accompanying z-pole ahead the arbor of cylindrical channel hose .

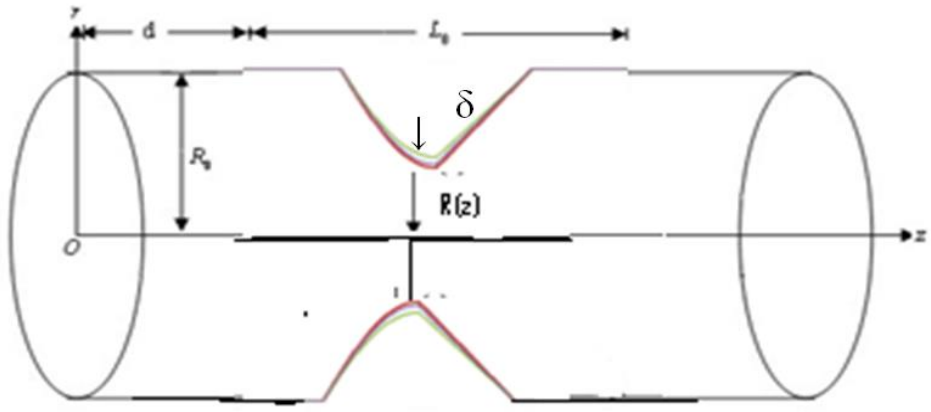

Figure 1: Arterial flow gadget and geometry.

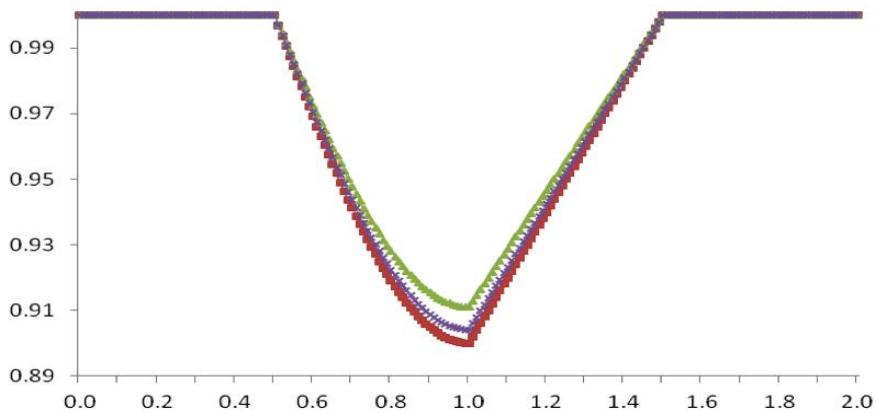

Figure 2: Geometry of time dependent stenosis with varying time.

The non-dimensional form of the equations for the axial variable, radial variable, radial rate of change, time, radial velocity, axial velocity and pressure are obtained by using $L_0, R_0, \delta, \delta^2/\nu_0, U, W$ and $L_0\mu_0 W/\delta^2$ as scales, respectively. Here μ_0 is the energetic thickness, $\nu_0 = \mu_0/\rho$ is the kinematic viscosity, ρ could be a reference thickness.

The most extreme speed within the pivotal course W is the one-dimensional fully-developed stream in a tube. U is the radial haste scale chosen as $\delta W/L_0$, which is set up by balancing terms in the mass durability equation. We have assumed mild stenosis $\delta \langle\langle R_0$, the diameter of the tube $2R_0$ of the same order as L_0, and sufficiently small $\left(\delta/L_0\right) R_e \langle\langle 1$,where R_e is the Reynolds number $R_e = 2\delta/\nu_0$.

Under these hypotheticals, the governingnon-dimensional equations are studied in this paper. We have taken $R_0 = 1$ mm. $L_0 = 1mm.\ d = 0.05mm.\ \delta = 0.01mm$ (or 0.03 mm), $W = 10mm/s$, $R_e = 0.3\langle 1$ and so $\left(\delta/L_0\right) R_e \langle\langle 1$ in accordance to the physiological conditions given by MeDonald, and Milnor, r and z are non-dimensional spatial variables for simplicity of memorandum.
The governing non-dimensional equations for unsteady dimensional laminar blood glide in the presence of a moderate stenosis case are considered under practical situations. The Reynolds number is sufficiently small, the most top ε of the stenosis is small ($\varepsilon = (3\delta)/(4R_0) \langle\langle 1$) and the axial scale L_0 is of the same order as the diameter $2R_0$ of the tube. They are :

$$\frac{\partial(ru)}{\partial r} + \frac{\partial(rw)}{\partial z} = 0 \qquad (1a)$$

$$\frac{\partial p}{\partial r} = 0 \qquad (1b)$$

$$\frac{\partial w}{\partial t} + \frac{\partial p}{\partial z} + \frac{1}{r}\frac{\partial(r\tau)}{\partial r} = 0 \qquad (1c)$$

The non-dimensional boundary conditions are:

$u = w = 0$ on $r = R(z, t)$ (1d)

$$\frac{\partial w}{\partial r} = 0 \text{ on } r = 0 \qquad (1e)$$

Where the shear stress τ is given by:

$$\tau = \left(-\frac{\partial w}{\partial r}\right)^n \qquad (1f)$$

p is the modified pressure, *u* is the radial component of the flow velocity, *w* is the axial component of the flow velocity, and *t* is the time variable. $\frac{\partial w}{\partial r}$ is the shear strain rate of the velocity gradient perpendicular to the plane of shear and n is the flow behavior index. There is no yield stress τ_0 so the equation does not model situation where there is a finite shear stress required to overcome viscosity and start flow. The Power-Law fluid model can be subdivided into three different type of fluids based on the value of their flow behavior index as follows; $n < 1$ pseudoplastic (shear-thinning fluids); $n = 1$ Newtonian fluid, and $n > 1$dilatants.

$R(z,t)$ is shape function for the radial structure of the inside boundary of the tube. Its unsteady extension of the steady form is given by:

$$R(z,t)=\begin{cases}1+2\varepsilon\left(1-\gamma e^{-t\alpha}\right)\left[\left(z-b-1\right)\right], & b+\frac{1}{2}\le z\le b+1\\ 1-\varepsilon\left(1-\gamma e^{-t\alpha}\right)\left\{\sin[\pi\left(z-b\right)]\right\}, & b\le z\le b+\frac{1}{2}\\ 1, & otherwise\end{cases} \quad (1g)$$

Where $\varepsilon=\frac{3\delta}{4R_0}$ tube $R_0=$radius of tube ,δ=max projection of strenosis, $0<\gamma\le 1$is unsteady parameter, $b=\frac{d}{L_0}$, $L_0=$length of stenosis , $d=$ indicates location where stenosis begins. Note that the max (critical) height of stenosis is at $z=b+0.5,$ Also $0<\varepsilon\le 1.0$.

Let $R=R_0+\gamma R_1 e^{-t\alpha}$ (1h)

Where

$$R_0(z)=\begin{cases}1-\varepsilon\sin\left[\pi\left(z-b\right)\right], & b\le z\le b+0.5\\ 1+2\varepsilon\left[\left(z-b-1\right)\right], & b+0.5\le z\le b+1.0\\ 1, \ otherwise & 0\le z\le b,\ b+1.0\le z\le 2b+1.0\end{cases} \quad (1i)$$

$$R_1(z)=\begin{cases}\varepsilon\sin\left[\pi\left(z-b\right)\right], & b\le z\le b+0.5\\ -2\varepsilon\left[\left(z-b-1\right)\right], & b+0.5\le z\le b+1.0\\ 0, & otherwise\end{cases} \quad (1j)$$

At stenosis throat, $z=b+\frac{1}{6}$, $z=b+\frac{5}{6}$

We write

$$(p,\ u,\ w)=\left[p_0(z),\ u_0(r,z),\ w_0(r,z)\right]+\gamma e^{-\alpha t}\left[p_1(r,z),\ u_1(r,z),\ w_1(r,z)\right], \quad (1k)$$

$\alpha=\alpha_r+i\alpha_i$ is a complex constant. Subscript "0" are the steady components of the dependent variables and those are subscript "1" are unsteady components of the dependent variables r and z.

2.1 Steady Case: $\left[u_0(\mathrm{r,z}),\ \mathrm{w}_0(r,z),\ p_0(z)\right]$

$$\frac{1}{r}\frac{\partial(ru_0)}{\partial r}+\frac{\partial(\mathrm{rw}_0)}{\partial \mathrm{z}}=0$$

(2a) $\frac{\partial p_0}{\partial r}=0$ (2b) $\frac{\partial p_0}{\partial z}+\frac{1}{r}\frac{\partial}{\partial r}\left[r\left(-\frac{\partial w_0}{\partial r}\right)^n\right]=0$

(2c)

The non-dimensional boundary conditions are:

$u_0=w_0=0$ on $r=R_0(z)$ (2d)

$\frac{\partial w_0}{\partial r}=0$ on $r=0$ (2e)

$$R_0(z)=\begin{cases}1-\varepsilon\sin\left[\pi(z-b)\right], & b\le z\le b+0.5\\ 1+2\varepsilon\left[(z-b-1)\right], & b+0.5\le z\le b+1.0\\ 1, \ \ otherwise & 0\le z\le b,\ \ b+1.0\le z\le 2b+1.0\end{cases} \quad (2f)$$

At stenosis throat:

$$z=b+1/6 \quad (3a)$$

From (2c) we have:

$$-\frac{\partial}{\partial r}\left[r\left(-\frac{\partial w_0}{\partial r}\right)^n\right]=r\left(\frac{\partial p_0}{\partial z}\right), \quad (\text{n is a positive number}) \ (3b)$$

Integrate with respect to r both side, we get:

$$\left(-\frac{\partial w_0}{\partial r}\right)^n=-\frac{r}{2}\frac{dp_0}{dz}$$

$$-\frac{\partial w_0}{\partial r}=\left(-\frac{1}{2}\frac{dp_0}{dz}\right)^{\frac{1}{n}}.r^{\frac{1}{n}} \quad (3c)$$

Again integrate with respect to r and use boundary condition at $r=R_0$, we get:

$$w_0(\mathrm{r},\mathrm{z})=\left(-\frac{1}{2}\frac{dp_0}{dz}\right)^{1/\mathrm{n}}\left(\frac{n}{n+1}\right)\left[R_0^{(n+1)/n}-r^{(n+1)/n}\right] \quad (4a)$$

Volume flow rate:

$$Q_0=2\pi\int_0^{R_0(z)}rw_0dr$$

$$Q_0=2\pi\int_0^{R_0(z)}rw_0dr=\pi\left(-1/2\frac{dp_0}{dz}\right)^{1/n}\left(\frac{n}{n+1}\right)\left(\frac{n+1}{3n+1}\right)R_0^{(3n+1/n)} \quad (4b)$$

Using (4b), we have

$$\frac{dp_0}{dz}=-2\left[\frac{(3n+1)Q_0}{\pi n}\right]^n\frac{1}{R_0^{(3n+1)}} \quad (4c)$$

Pressure drop:

$$p_0=-\int_0^{1+2b}\left(\frac{dp_0}{dz}\right)dz=p_0(0)-p_0(1+2b) \quad (4d)$$

Flow resistance (impedance):

$$\lambda_0=\frac{\Delta p_0}{Q_0} \quad (4e)$$

Wall shear stress:

$$\tau_{w_0}=-\frac{R_0}{2}\frac{dp_0}{dz} \quad (4f)$$

Shear stress at the stenosis throat is:

$$\tau_{w_0}\Big|_{R_0}=1-\varepsilon$$

Frictional; force on the wall of artery is:

$$F_0=2\pi\int_0^{1+2b}\tau_{w_0}dz \quad (4g)$$

Radial velocity:

$$u_0=-\frac{1}{r}\int_{R_0}^{r}\left(\frac{\partial w_0}{\partial z}\right)dr \quad (4h)$$

2.2 Unsteady case:

Use (1k) and (1f) in (1c), we assume $0<\gamma\le 1$ and zeroth order in γ, we have equations and results for w_0, p_0 etc given in above.

We apply a Taylor series expansion for boundary conditions for $w(z,r,t)$ at $r=R_0$

$$w\big|_{r=R}=0=w\big|_{r=R_0}+\gamma e^{-\alpha t}R_1(z)\frac{\partial w}{\partial r}\Big|_{r=R_0}+0\left(\gamma^2\right) \quad (5a)$$

It is valid for $\gamma<<1$.

In the order one of γ, we find from ((1c-1e) [after (1k) and (1f) are used in (1c-1e)] and after we divide each equation by $\gamma e^{-\alpha t}$

$$-\alpha w_1=-\frac{dp_1}{dz}-\frac{1}{r}\frac{\partial}{\partial r}\left\{\left\{r\,n\left(-\frac{\partial w_0}{\partial r}\right)^n\left(-\frac{\partial w_1}{\partial r}\right)\right\}\right. \quad (5b)$$

$$w_1=R_1\frac{\partial w_0}{\partial r} \text{ at } r=R_0(z) \quad (5c)$$

$$\frac{\partial w_1}{\partial r}=0 \text{ at } r=0 \quad (5d)$$

To derive additional equations (we have two unknowns w_1 and p_1, we need two equations for these unknowns), we make use of volume flow rate. Write

$Q=Q_0+\gamma e^{-\alpha t}Q_1$ (5e)

Where Q_0 is for steady case of Q given by equation (4b)and

$$\begin{aligned}Q&=2\pi\int_0^{R(z,t)}rw\,dr\\&=2\pi\int_0^{R_0+\gamma e^{-\alpha t}R_1}r(w_0+\gamma e^{-\alpha t}w_1)dr\\&=2\pi\int_0^{R_0}r\,w_0\,dr+2\pi\int_0^{R_0+\gamma e^{-\alpha t}R_1}r\,w_0\,dr+\left[2\pi\int_0^{R_0}r\,w_1\,dr\right]\left(\gamma e^{-\alpha t}\right)+O\left(\gamma^2\right)\end{aligned}$$

(5f) Thus

$$Q_1=2\pi\int_0^{R_0}rw_1dr+\frac{1}{\left(\gamma e^{-\alpha t}\right)}\int_{R_0}^{R_0+\gamma e^{-\gamma t}R_1}rw_0dr \quad (5g)$$

Q_1 is the initial volume flow rate due to the oscillatory part. Prescribing Q_0 and Q_1 (given γ, α and t),then Q has some value, which is assumed to be given.

Now we multiply (5b) by r , 2π , integrate in r from r = 0 to R_0 , we have

$$-\frac{\alpha Q_1}{2\pi}=-\left(\frac{R_0^2}{2}\right)\frac{dp_1}{dz}-R_0n\left[\left(\frac{\partial w_0}{\partial r}\right)^{n-1}\left(-\frac{\partial w_1}{\partial r}\right)\right]\Big|_{r=R_0} \quad (5h)$$

We have from equation (5b)

$$-\alpha w_1=-\frac{dp_1}{dz}+A\frac{\partial w_1}{\partial r}+B\frac{\partial^2 w_1}{\partial r^2}$$

$$A=\frac{(2n-1)}{r^{1/n}}\left(-\frac{dp_0}{dz}\right)^{(n-1)/n},\quad B=n\left(-\frac{1}{2}\frac{dp_0}{dz}\right)^{(n-1)/n} r^{(n-1)/n} \quad (5i)$$

Using equations (5h) we have:

$$\frac{\partial^2 w_1}{\partial r^2}=\bar{p}\frac{\partial w_1}{\partial r}+\bar{q}w_1+\bar{r} \quad (5j)$$

where $\bar{p}=\frac{C-A}{B}$, $\bar{q}=\frac{\alpha}{B}$, $\bar{r}=-\frac{\alpha Q_1}{\pi B R_0^2}$ (5k)

and $C=\frac{2n}{R_0^{1/n}}\left(-\frac{1}{2}\frac{dp_0}{dz}\right)^{(n-1)/n}$ (5l)

The values given for system w_0 in steady state (5b-5d) and (5h) can be resolved numerically. A staggered finite difference grid is utilised about that boundary to ensure second order correctness of the Neumann (derivative) boundary condition at $r=0$ In other words, the r values must be outside of the region where $r=0$. In order to generate a linear system of equations of the type $Aw=d$, where A is a N by N tridiagonal matrix and w and d are vectors of dimension N, we discretized the differential equation governing the behaviour of w_i where $i\in\{2,3.....N-1\}$.

The equations were solved using a subroutine. This subroutine uses row interchanges, partial pivoting, and Gaussian elimination to solve the equations and get p_1 and w_1 . Then, using these in (1k), we can find w and p , and u can be found from

$$u=-\frac{1}{r}\int_R^r r\left(\frac{\partial w}{\partial z}\right)dr \quad (5m)$$

3. Results and Discussion:

The calculation of the axial velocity field, pressure gradient, impedance (resistance), and wall shear stress takes into account many numerical factors that are relevant to the situation at hand in order to better understand the physical characteristics of blood flow in an artery with a time-dependent stenosis. For this we start from $\varepsilon=0.1,0.04\le 1$ (maximum height of the stenosis), the frequencies $(\alpha_r=0,-1,-2,-3)$, $(\alpha_i=0,1,2,3)$, Q = 1 and from $\gamma=0.3$.

The results presented in this section appear to be typical of all the computational data, we have collected at various parameter values.

3.1 Axial velocity (figure 1: velocity in the z-direction)

Figure 3 -6 displays the estimated axial velocity w for several scenarios. Figures 3 and 4 show the axial velocity against n time variables for various frequencies $\alpha_r=0,-1,-2,-3,\alpha_i=0$ or 1, at $z=1,r=0.5,\gamma=0.3$ and $\varepsilon=0.1$ and 0.3, respectively presented in Figure 3- Fig.-4.

The findings for the velocity profile of the blood flow at the stenosis throat ($z=0.67$) for various values of the flow behavior index (n) are shown in Figure -3. Now Figure -4 is identical to Figure 3, but with $\varepsilon=0.03$ instead. Axial velocity is shown to increase as flow behavior index (n) increases. In other words, axial velocity increases with time and is larger for Newtonian fluid (n = 1) than for non-Newtonian fluid (n 1). Figures- 3 and 4 demonstrate that the featured curves are similar in that as one proceeds away from the axis, they gradually expand until they reach the maximum at t = 1.

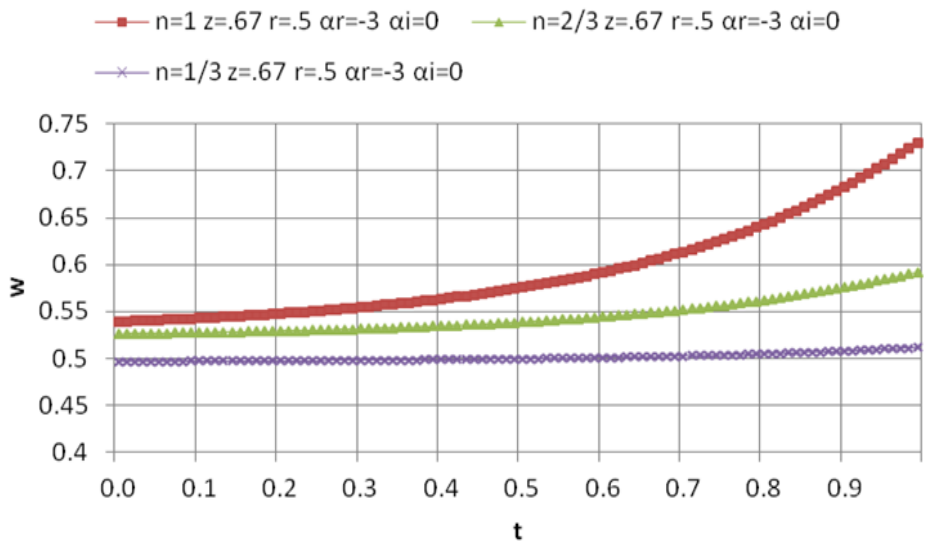

Figure 3: Axial velocity versus time variable for different values of $\alpha_r = -3$ $\alpha_i = 0$ and for $\varepsilon = 0.1, r = 0.5, z = 0.67, \gamma = 0.3, n = 1,\ 2/3, 1/3$.

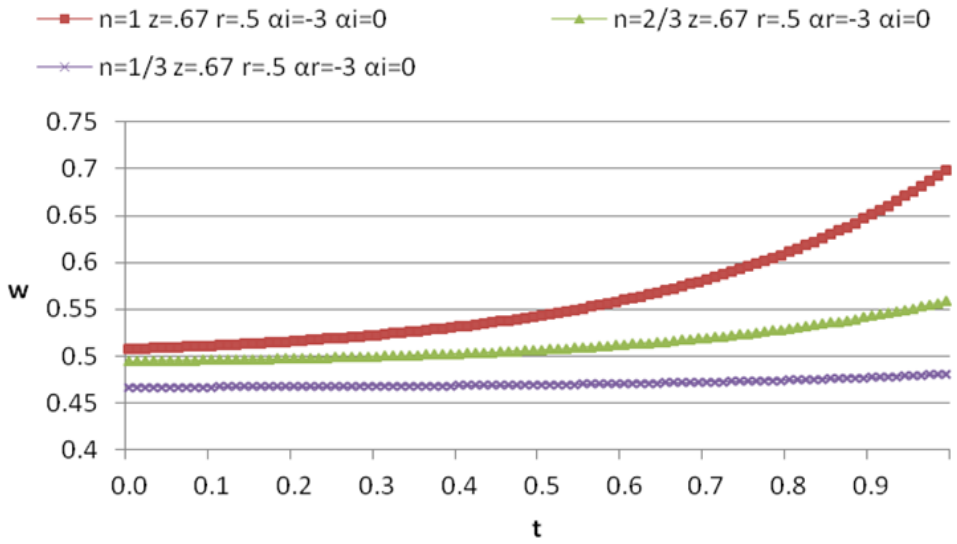

Figure 4: Shows the axial velocity as a function of time for various values of the parameters $\varepsilon = 0.03, r = 0.5, z = 0.67, \gamma = 0.3, n = 1,\ 2/3, 1/3$ and $\alpha_r = -3, \alpha_i = 0$.

The axial velocity grows in size as the frequency grows (for brevity, not illustrated). As can be seen in Figures- 3 and 4, the magnitudes of axial velocity rise as the height of the stenosis increases. The axial velocity at $z = 0.67$ for $r = 0.75$ is computed using the same numbers as in Figures -3 and 4, and it is discovered that the magnitude of the axial velocities is less for $r = 0.5$ (for brevity, figures are not provided).

As the radial variable rises, the magnitude of the axial velocity decreases, as demonstrated in Figures-5 and 6. Axial velocity is seen to grow as the flow behaviour index (n) increases and reach a maximum at r = 0. It then progressively drops with an increase in artery radius (r) and achieves a minimum value at the stenotic wall $\left(r = R(z)\right)$ for all scenarios taken into consideration. The axial velocity vs the radial variable for various frequencies at z = 0.67 (stenosis mouths) and z = 1 (critical height) for $t = 1, \gamma = 0.3$ and $\varepsilon = 0.1$ are shown in Figures- 5 and 6. Figure 6 is identical to Figure-5 with the exception that z = 1. Axial velocities at z = 1 are greater than those at z = 0.67. The results show that the axial velocity can drop to virtually zero very close to either the stenosis throat or the critical height, which indicates that there is significant friction affecting the flow in the area around the stenosis.

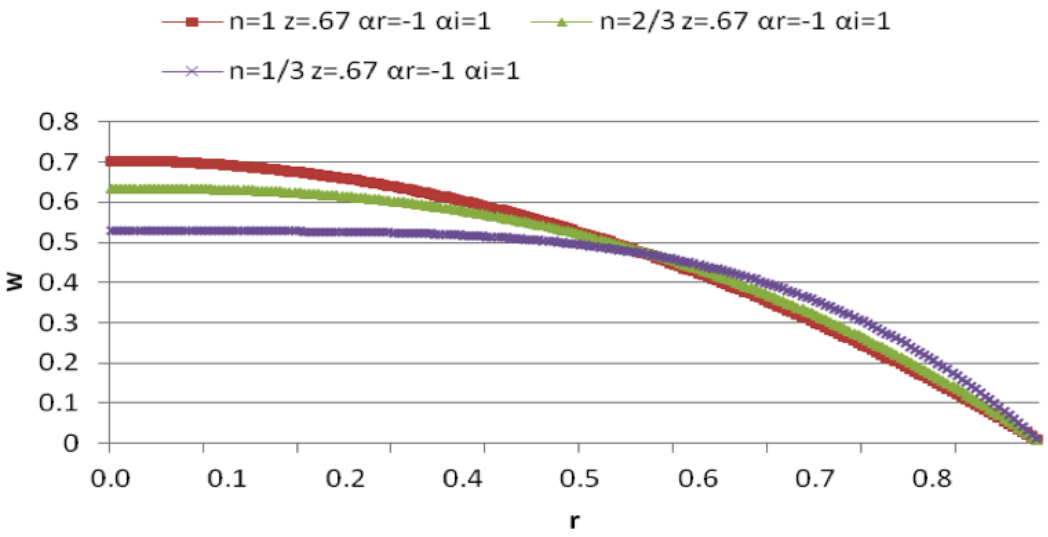

Figure-5 : Shows the relationship between axial velocity and radial variable for various values of $\varepsilon = 0.1, \mathrm{z} = 0.67, \gamma = 0.3, \mathrm{n} = 1,\ 2/3, 1/3$ and $\alpha_r = -3, \alpha_i = 1$

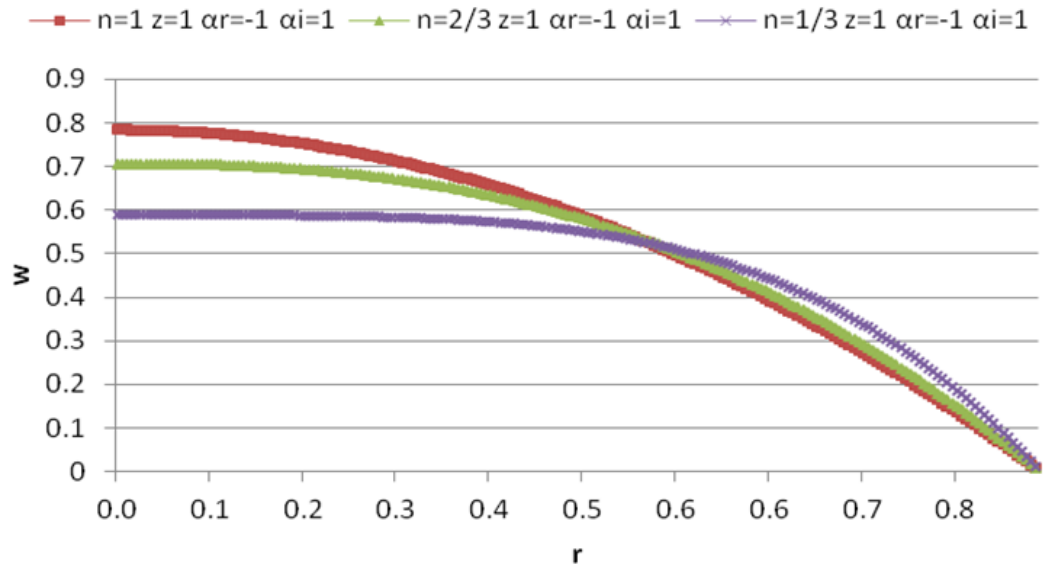

Figure 6: Shows the axial velocity vs the radial variable for different values of $\alpha_r = -3, \alpha_i = 1$ as well as for $\varepsilon = 0.1, \mathrm{z} = 1.0, \gamma = 0.3, \mathrm{n} = 1,\ 2/3,\ 1/3.$

Our further produced data at the second stenosis throat's axial position $z = 1 + 5/6$ showed that the pressure gradient, impedance, and wall shear stress values were almost identical to those at the first stenosis throat ($z = 0.5 + 1/6$).

3.2 Pressure gradient (rate of change of pressure along the z-direction, Figure 1)

Figures 7 and 8 shows the pressure gradient's fluctuation versus axial distance for various values of the frequencies $\alpha_r = 0, -1, -2, -3$, $\alpha_i = 0, 1, 2, 3, Q = 1, \gamma = 0.3, n = 2, t = 1$ and $\varepsilon = 0.1$. With the exception of $\alpha_r = -3$, Figure 8 is identical to Figure 7. These figures show that the pressure gradient is negative, which means that as the axial variable rises, the pressure force drops. Additionally, it should be noted that in all circumstances taken into consideration, the pressure gradient has its greatest magnitude at the critical height of stenosis, but the pressure gradient is uneven throughout the stenosis area and constant beyond the stenosis zone. The narrowest passage of the outline of the stenosis gives rise to maximum magnitude of pressure gradient for the Newtonian and non-Newtonian fluid cases. The pressure gradient distributions show a close

mirror image of the outline of the stenosis. The higher the frequency, the higher the magnitude of the pressure gradient is. We computed pressure gradient with different values of ε and it is observed that as the size of the stenosis increases, the magnitude of the pressure gradient also increases. That is, more severe stenosis can lead to higher blood pressure force in the artery. This result will be useful for medical purpose.

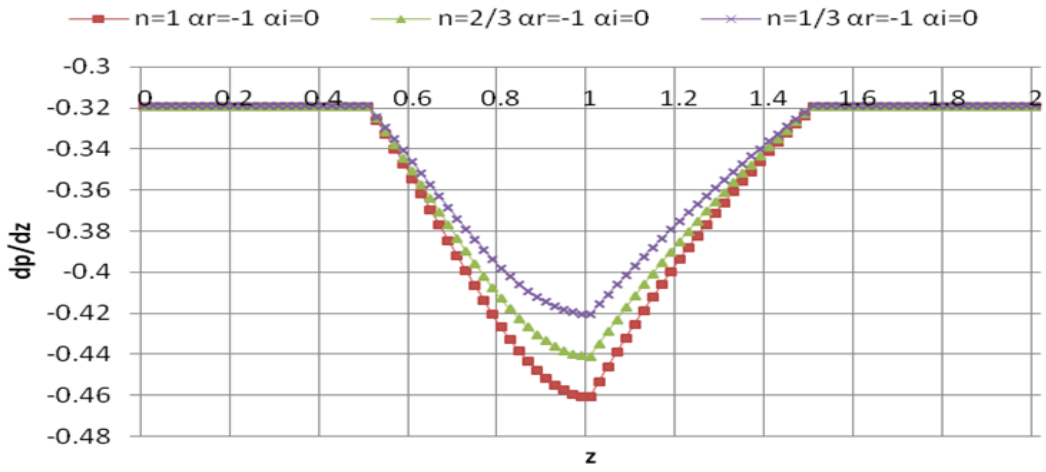

Figure 7. Pressure gradient as a function of z for $\gamma = 0.3$, e=0.1, n=1, 2/3, 1/3, t=1 and for several values $\alpha_r = 1,\ \alpha_i = 0$.

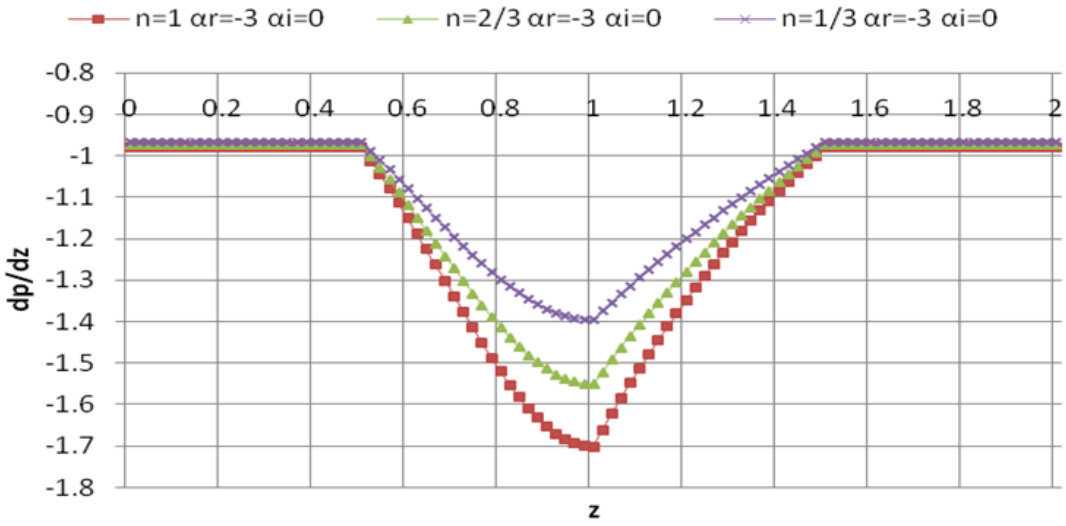

Figure 8: Pressure gradient versus *z* for $\gamma = 0.3$, *e* =0.1, n=1, 2/3, 1/3, *t*=1 and for several values of $\alpha_r = -3$, $\alpha_i = 0$.

3.3 Wall shear stress:

Because the cut stress on the arterial obstruction allocation is a main diagnostic determinant to try characteristic of ancestry flow through the channels, we have checked the obstruction cut stress for various principles of the commonness and several various cases are bestowed in Figure 9 - 12.

The divider cut stress against moment of truth changing for different principles of the repetitions $\alpha_r = 0, -1, -2, -3, \alpha_i = 0, 1, 2, 3$ and for $\gamma = 0.3, \varepsilon = 0.1$, and z = 0.5+1/6 and 1, are bestowed in composite Figure- 9 -10. Figure-10 is the same Figure-9, except for z=1. The importance of the divider cut stress is higher at detracting climax than at the blockage neck. The maximum advantage of the obstruction cut stress takes place for best index worth (n) at t = 1. For very small recurrences, it takes a significantly very long time before obstruction clip stress can enhance abundant and meaningful (for briefness not shown). The curves promoted are identical in the sense that they increase from their individual minimum at the axle all at once moves away it and permanently reach their maximum at t = 1. From our supplementary dossier we noticed that the obstruction cut stress increases as the amount of the blockage raised.

The divider clip stress against the principal distance for various principles of the recurrences $\alpha_r = 0, -1, -2, -3, \alpha_i = 1, \beta = 0.3, Q = 1, \gamma = 1, t = 1$ and $\varepsilon = 0.1$ and 0.03 are bestowed in Figure 11 -12. Figure-12 is the same Figure-11, except the profit of ε is 0.03. It is noticed that divider cut stress increases as flow conduct index (n) increases. That is, the obstruction cut stress is less for non-Newtonian than Newtonian ancestry flow for a likely blockage magnitude.

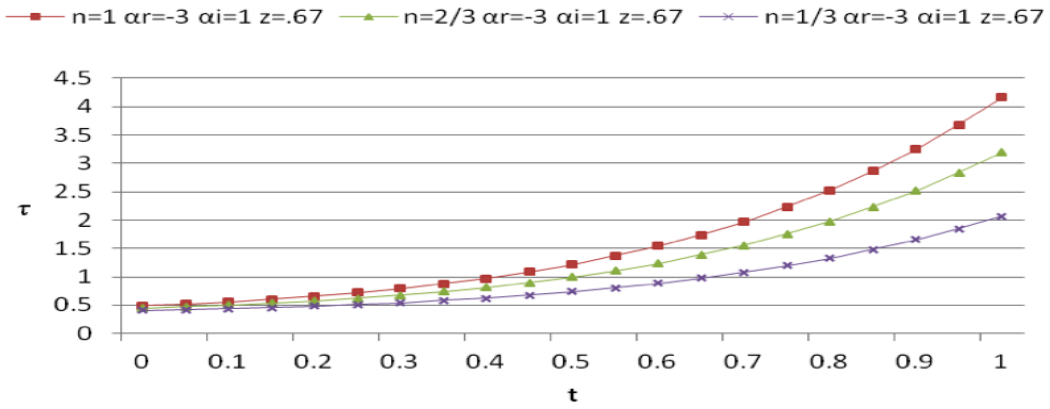

Figure 9. : Wall shear stress versus t for $\varepsilon = 0.1, n = 1, \frac{2}{3}, \frac{1}{3}, z = 0.67 \gamma = 0.3$ and for various principles of the repetitiveness $\alpha_r = -3 \alpha_i = 1$.

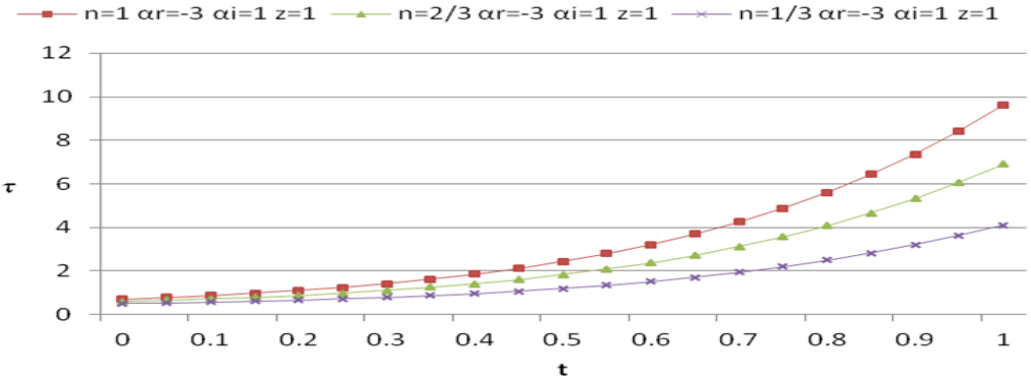

Figure 10: Wall shear stress versus t for $\varepsilon = 0.1, n = 1, \frac{2}{3}, \frac{1}{3}, z = 1.0, \gamma = 0.3$ and for various values of the repetitiveness $\alpha_r = -3 \alpha_i = 1$.

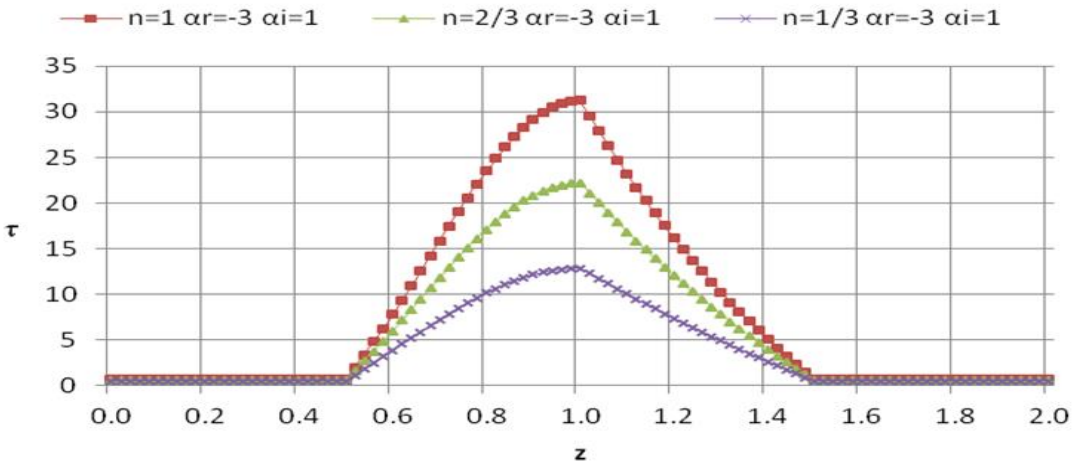

Figure 11: Wall shear stress versus z for $\varepsilon = 0.1, n = 1, \frac{2}{3}, \frac{1}{3}, \gamma = 0.3, t = 1$ and for various values of the repetitiveness $\alpha_r = -3 \alpha_i = 1$

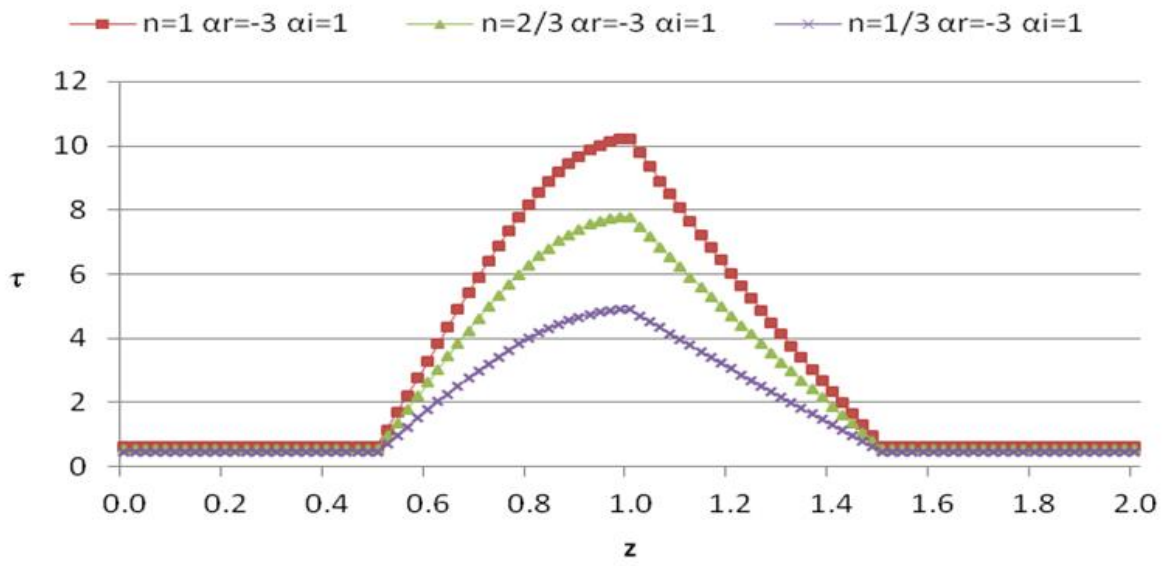

Figure 12: Wall shear stress versus z for $\varepsilon = 0.03, n = 1, \frac{2}{3}, \frac{1}{3}, \gamma = 0.3, t = 1$ and for various values of the repetitiveness $\alpha_r = -3\alpha_i = 1$

It may be visualized that the divider shear stress is determined and certain in the domain outside the blockage district, indicating the existence of a definite and never ending force performed for one elapse the channel. The wall cut stress distributions show a close exact counterpart of the outline of the blockage.

In the blockage district, the stress force is changeable and higher than that outside blockage district. Higher repetitiveness leads to taller clip stress accompanying its peak profit at detracting altitude. The narrowest transition of the outline of the blockage gives make even the best obstruction cut stress for the Newtonian and non-Newtonian fluid cases.

As anticipated, the magnitudes of clip stresses are larger as the blockage breadth increases proved in Figure 11 and Figure 12.

Thus resolving the results, individual can decide the divider cut stress changes with the order reversed accompanying the amplitudes of pressure slope.

The study of the stress distributions of the arterial surround the neighbourhood of a blockage is main. It will help us to expound the cause of post-stenotic extension (the extension of the arterial divider urgently coming after of a blockage) and the growth and progress of arterial blockage.

3.4 Impedance (Resistance)

When stenosis develops in an artery, one of the most serious issues is the increased resistance (impedance) and the associated reduction of the blood inflow by the roadway to the particular vascular bed.

Figure 13- Figure 14 present the impedance versus time variable for several values of the frequencies, for $\varepsilon = 0.1$ and 0.03, independently.

The angles featured are analogous in the sense that they increase from their individual minimum at the axis as one moves down from it and eventually reaches the outside at t = 1. It can be seen from these numbers that the impedance is non-negative and it increases as in flow behaviour indicator (n) increases. It's set up that the difference in the magnitude of impedance between Newtonian and non-Newtonian fluid increases with the stenosis height. It's clear from the description of impedance that under a given pressure grade, a lesser impedance will indicate lower inflow of fluid.

Therefore the impedance gives a measure of the volume of blood entered by different organs. Hence this is an important factor which might play a vital part in the opinion and treatment of heart attack and stroke.

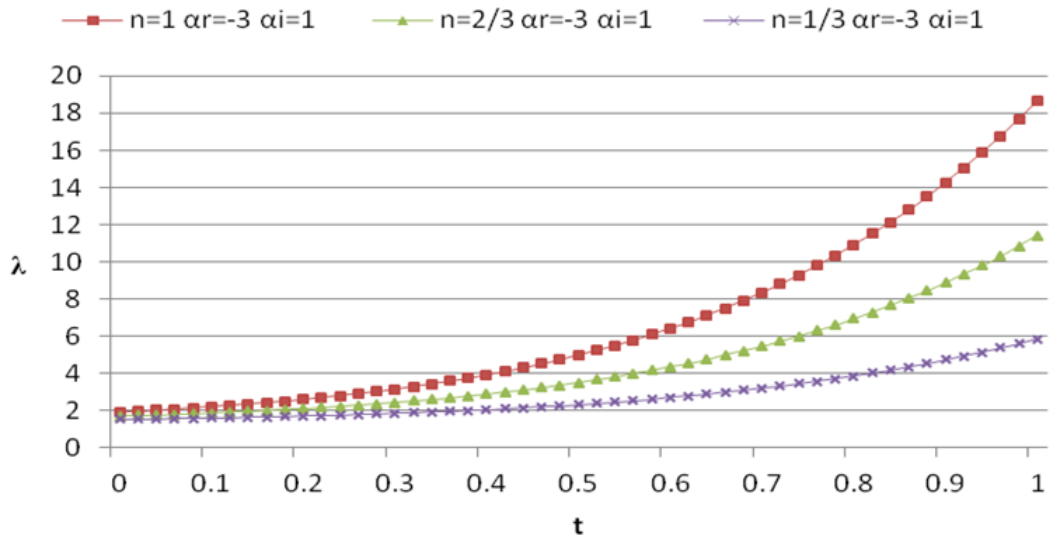

Figure 13: Impedance versus t for $\varepsilon = 0.1, n = 1, \frac{2}{3}, \frac{1}{3}, \gamma = 0.3$ and for various principles of the repetitiveness $\alpha_r = -3 \alpha_i = 1$.

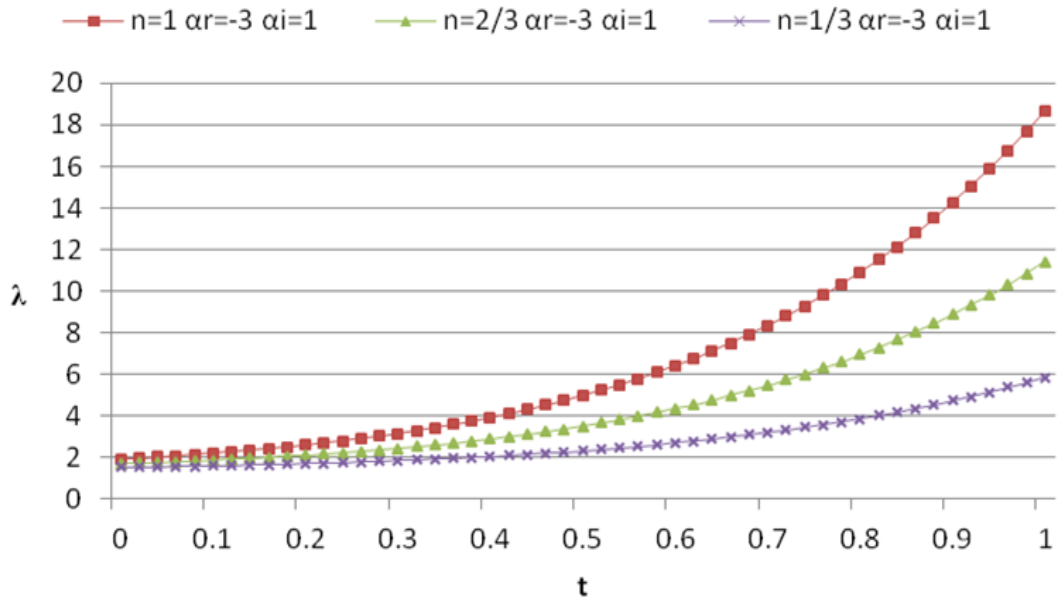

Figure 14: Impedance versus t for $\varepsilon = 0.03, n = 1,\ 2/3,\ 1/3,\ \gamma = 0.3$ and for various principles of the repetitiveness $\alpha_r = -3,\ \ \alpha_i = 1$.

4. CONCULATION:

The study examined unsteady arterial blood flow in time-dependent stenosis using the non-Newtonian Power-Law blood fluid flow model. It calculated pressure gradient, flow velocity, impedance, and wall shear stress for steady and unsteady cases at critical heights and throats**.** The study evaluated various frequencies, power index numbers, and stenosis height parameters. Results showed that pressure gradient, flow velocity, wall shear stress, and impedance are higher in the stenosis zone than non-stenosis zones. These parameters also increase as stenosis height increases. Newtonian fluid (n=1) has higher magnitudes than non-Newtonian fluid (n<1) and increases with time. Additionally, flow velocity, pressure gradient, impedance, and wall shear stress increase significantly as frequency increases. This study highlights the importance of unsteadiness in wall shear stress, emphasizing the oscillation effect. The maximum value coincides with flow rate and varies inversely with pressure gradient amplitudes. The mathematical model predicts interesting hemodynamic features for physiologists.

REFERENCES

1. Young, D. F. and Tsai, F. Y. (1973). Flow characteristics in models of arterial stenoses in steady flow, J*ournal of Biomechanics*, 6 (4), 395–410.
2. Nadeem, S., Akbar, N. S., Hendi, A. A., and Hayat, T. (2011). Power law fluid model for blood flow through a tapered artery with a stenosis. *Applied Mathematics and Computation*, 217(17), 7108-7116.
3. Nasrin, R., Hossain, A., and Zahan, I. (2020). Blood flow analysis inside a stenotic artery using power-law fluid model, *Research and Development in Material Science*, 13(1), 1360-1368.
4. Texon, M. (1960). The hemodynamic concept of atherosclerosis, *Bulletin of the New York Academy of Medicine*, 36(4), 263.
5. Young, D. (1968). Effect of a time-dependent stenosis on flow through a tube, Journal of Engineering for Industry, vol. 90, no. 2, pp. 248–254, 1968.
6. Morgan, B. E., and Young, D. F. (1974). An intergral method for the analysis of flow in arterial stenoses, *Bulletin of Mathematical Biology*, *36*, 39-53.
7. Taylor, M. G. (1959). The influence of the anomalous viscosity of blood upon its oscillatory flow, *Physics in Medicine and Biology*, *3*(3), 273.
8. MacDonald, D. A. (1979). On steady flow through modelled vascular stenoses, *Journal of biomechanics*, *12*(1), 13-20.
9. Hershey, D., Byrnes, R. E., Deddens, R. L. and Rao, A. M. (1964). Blood rheology: Temperature dependence of the power law model, *AI Ch. E. Boston*.
10. Huckabe, C. E., and Hahn, A. W. (1968). A generalized approach to the modeling of arterial blood flow, *The Bulletin of mathematical biophysics*, *30*, 645-662.
11. Neofytou, P. and Tsangaris, S. (2006). Flow effects of blood constitutive equations in 3D models of vascular anomalies, *International journal for numerical methods in fluids*, *51*(5), 489-510.
12. Chan, W. Y. Ding, Y. and Tu, J. Y. (2005). Modeling of non-Newtonian blood flow through a stenosed artery incorporating fluid-structure interaction, *Anziam Journal*, *47*, C507-C523.
13. Cho, Y. I. and Kensey, K. R. (1991). Effects of the non-Newtonian viscosity of blood on flows in a diseased arterial vessel. Part 1: Steady flows, *Biorheology*, *28*(3-4), 241-262.
14. Mandal, P. K. (2005). An unsteady analysis of non-Newtonian blood flow through tapered arteries with a stenosis, *International Journal of non-linear Mechanics*, *40*(1), 151-164.
15. Chakravarty, S., and Mandal, P. K. (1994). Mathematical modelling of blood flow through an overlapping arterial stenosis, *Mathematical and Computer Modelling*, *19*(1), 59-70.
16. Fry, D. L. (1968). Acute vascular endothelial changes associated with increased blood velocity gradients, *Circulation Research*, 22(2), 165-197.
17. Rakshit, S., Agrawal, B., and Kumar, S. (2023). A mathematical model of flow of blood in a segment of an artery by a non-homogenous approach, Journal of Data Acquisition and Processing, 38(1), 5495.
18. Agrawal, B., Kumar, S. and Rakshit, S. (2022). A mathematical study of constrained fluid movement in the arterial system due to the formation of multiple stenosis, *IJAR*, *8*(3), 455-464.
19. Kumar Mandal, P., Chakravarty, S. and Mandal, A. (2007). Numerical study of the unsteady flow of non-Newtonian fluid through differently shaped arterial stenoses, *International Journal of Computer Mathematics*, *84*(7), 1059-1077.
20. Chaturani, P. and Palanisamy, V. (1990). Casson fluid model for pulsatile flow of blood under periodic body acceleration, *Biorheology*, *27*(5), 619-630.